

Optical bench for chemical laser testing

D. S. L. Durie

Bell Aerospace Textron
Division of Textron Inc.
P.O. Box One
Buffalo, New York 14240

Abstract. An optical bench for developmental testing of chemical laser hardware is described. It is specially designed to withstand the vibration and thermal disturbances inherent in this type of laser, and has universal features which enable it to accept a variety of nozzle and mirror sizes. The paper deals with the adaptation of traditional designs to meet new requirements in the areas of bench deflection, adjustable mirror mounts, and remote mirror actuation for closed cavity power measurements. In particular, a noncantilever mount with offset pivot for heavy mirrors is described.

Keywords: lasers; chemical lasers; optical testing; optical bench; mirror mounts; closed cavity power.

Optical Engineering 20(4), 625-628 (July/August 1981).

CONTENTS

1. Introduction
2. Optical bench assembly
3. Mirror mount design
4. Analysis of offset pivot geometry
5. X_c actuation
6. References

1. INTRODUCTION

In laser design the problem of maintaining the alignment of resonator mirrors has always required careful consideration. This is especially true in high power chemical lasers in which the lasing medium consists of gases flowing at supersonic speeds with chemical reaction temperatures of the order of 2000 K. The resulting acoustic noise and thermal growth generated in the walls of the duct containing the gas flow are sufficiently disruptive to mirror alignment that no direct mechanical connection can be allowed between the duct and the optical bench. To obtain acoustic and thermal isolation, therefore, each must be individually supported from the floor of the test cell on an independent structure; the bench, in addition, must follow a circuitous path around the duct giving it a "U" shape. This is in contrast with the linear shape generally found in table-top gas lasers where the optical bench is in direct contact with all principal components of the laser system for which it acts as a general chassis.

In high power chemical lasers, the requirement that the mirrors be situated inside the laser envelope while the bench supporting them remains outside adds further complication to the bench design. One design approach employs mirror support structures that pass through ports in the walls of the laser envelope without making contact; at the same time, the ports must be sealed so that the near vacuum inside the laser is not disrupted. Mirror support structures must, in addition, resist forces generated by hoses conducting coolant to the mirrors, which protects them from the high incident power densities.

Paper 1702 received June 30, 1980; revised manuscript received Aug. 24, 1980; accepted for publication Aug. 28, 1980; received by Managing Editor Sept. 8, 1980.
© 1981 Society of Photo-Optical Instrumentation Engineers.

Finally, since the bench is used in an experimental testing facility for the development of nozzles and duct hardware, it should have a high degree of adaptability to allow a variety of nozzle arrays and mirror sizes to be installed with convenience. This convenience minimizes the time required for both setup and alignment prior to each test run which, in turn, maximizes actual testing time in any given test day. The designs of both optical bench and mirror mounts, therefore, bear directly on cost effectiveness of the whole test facility.

2. OPTICAL BENCH ASSEMBLY

The previously mentioned "U" shape of the bench assembly can be seen in Fig. 1. Each arm of the U consists of a steel pier and a three-post superstructure attached to its top surface. The base of the U is a seismic block to which the two piers are attached.

The seismic block, made of concrete, has outside dimensions of 305 × 91 × 91 cm with a resulting weight of approximately 5604 kg. It is surrounded by material which absorbs acoustic vibration transmitted from the laser nozzle and from the steam ejector system which generates vacuum for the laser device. Adequate accessibility is ensured for installation of pressure and temperature sensors in the underside of the laser duct by placing the seismic block below floor level.

Each pier rests on three steel inserts embedded in the concrete in a circular pattern spaced 120° apart. The inserts are tapped to receive bolts 2.5 cm in diameter which pass through holes in the circular flange which forms the lower end of the pier. This three point attachment follows kinematic principles aimed at providing strain-free supports for the mirror which are required to have angular stabilities approaching one second of arc.

The space between the piers must be adjustable to allow testing of laser hardware with a variety of widths. This is accomplished by installing several groups of inserts in the upper surface of the seismic block, with 25 cm intervals between the groups. This allows the piers to be moved in 25 cm increments to the left or right depending on the width of the nozzle array that must be accommodated. For this scheme to work successfully, the inserts must have female threads and their upper ends must lie in a plane which clears the concrete surface.

Thus far in the design, there has been little difficulty in making the

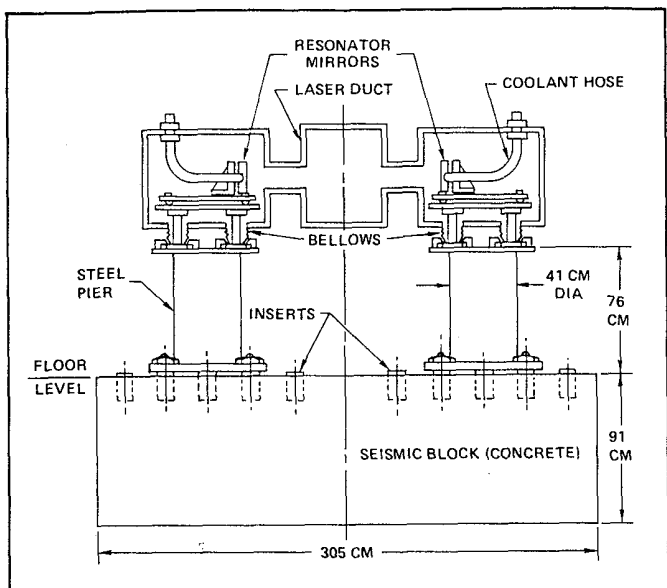


Fig. 1. Optical bench and mirror mounts.

optical bench stiff enough for its intended purpose. This has been accomplished through use of generous cross-sectional areas in both seismic block and the two piers, the latter, for instance, being made from 41-cm-diameter steel pipe. However, the question arises as to the best method of continuing the bench structure through the wall of a mirror box to a point where a mirror can be attached. The problem with simply extending the 41-cm-diameter pier through the wall is that, due to the vacuum inside the mirror box, atmospheric pressure tends to drive the pier into the box with a force proportional to the hole area, in this case 1545 kg. Since the presence of this level of force within a structure is not conducive to an angular stability of a few arcseconds, an alternative method was sought.

One approach is to continue the structure through the wall in the form of several posts of smaller diameter such that atmospheric pressure acting on the total of their areas creates a more modest force.

Since we desire the most strain-free design possible, the number of posts is limited to three in accordance with kinematic principles. Structural stiffness is enhanced by increasing the spacing between posts and by use of flanges on both top and bottom ends. Each post is then operating as a beam in the cantilever mode with the equivalent of "built-in," or fixed, attachments at both ends.

We are concerned principally with rotational stability of a mirror, particularly rotations about the altitude and azimuth axes. A multi-post arrangement is extremely stiff about the altitude axis because in that mode the posts experience only simple compression or tension forces. The azimuth mode is less stiff and therefore requires analysis of angular deflection resulting from an applied torque.

Figure 2(a) shows support plate P2 attached to three posts equispaced on a circle of radius R_p . The top flanges of the posts are bolted to P2. The bottom flanges are fastened to the pier surface by means of clamps which allow adjustment of P2 relative to the pier. To simulate a disturbing torque such as might be produced by a coolant hose, force F is shown at radius R_f from the center of the post pattern. This results in both translation and rotation of P2. As an aid to the analysis we can employ the theorem that states: A given force can be resolved into a coplanar force and a couple, the component force being equal and parallel to the given force, and the couple having a moment equal to that of the given force about any point in the line of action of the component force.

We choose the location of the component force such that it passes through the center of the post circle where it causes only translational movement, which is not of primary concern. The couple, however, produces rotational movement of P2. The magnitude of the couple is

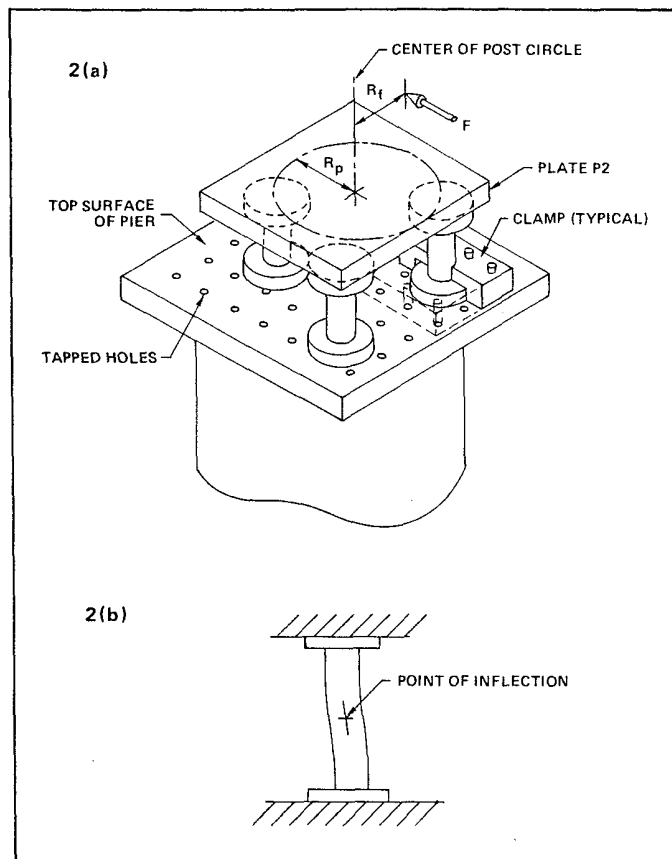


Fig. 2. (a) Application of eccentric force to three-post structure, and (b) bending shape of posts.

FR_f and it acts about the center of the post circle, thus producing equal bending in all posts. Equal twisting in all posts is ensured by their solid attachment to P2.

The basic task is to evaluate the effect of a couple FR_f applied about an axis passing through the center of the post circle. It transmits both a bending torque WR_p and a twisting torque T to each post such that, for three posts

$$FR_f = 3(WR_p + T) \tag{1}$$

where W is the tangential load on a single post.

The standard beam formula for the maximum bending deflection of a post is $Y = KWL^3/EI$ or, making it explicit in W , we have

$$W = YEI/KL^3 \tag{2}$$

Twisting of the same post is given by

$$T = JG\theta/L \tag{3}$$

Substituting Eqs. (3) and (2) into Eq. (1), we get

$$FR_f = 3(YEIR_p/KL^3 + JG\theta/L) \tag{4}$$

Substituting $Y = R_p\theta$, $I = \pi D^4/64$, $J = \pi D^4/32$ into Eq. (4) we get

$$\theta = FR_f(R_p^2ED^4/64KL^3 + D^4G/32L)^{-1} \times 1/3\pi, \tag{5}$$

where

$$\theta = \text{twist of each post and azimuth rotation of P2,}$$

FR_f = applied torque,

R_p = radius of post circle,

E = Young's modulus,

I = area moment of post,

J = polar area moment of post

K = constant depending on method of attaching post ends,

L = post length,

G = modulus of rigidity, and

D = post diameter.

Our objective is to minimize θ . In Eq. (5) the least value of θ is achieved by maximizing the numerator terms within the brackets and minimizing the denominators. Clearly, one of the most effective parameters is post diameter D due to its inclusion to the fourth power in both the bending and twisting expressions within the brackets. K is minimized by employing flanges at both ends of the posts.

Engineering handbooks do not give the value of K for a beam constrained in this fashion, i.e., a cantilever with the loaded end having zero slope. However, it can be derived by noting that each post is bent into the same shape as each half of a beam that is fixed at both ends and carries a concentrated load at the center. For the latter, $Y = WL^3/192EI$. If we equate the deflections of the half and full length beams, we can write

$$WL^3/192EI = K(W/2)(L/2)^3/EI \quad (6)$$

and $K = 1/12$.

We can now solve Eq. (5) for the stiffness of a three post structure with respect to the azimuth axis when unit torque is applied. For steel posts with $R_p = 19.0$ cm, $D = 5$ cm, $L = 20$ cm, and $FR_f = 1$ kg-cm, we obtain $\theta = 8.8 \times 10^{-9}$ radians/kg-cm.

In a perfect kinematic design, the post lengths would be identical, the flanges on each post would be perfectly square to the post axis, and the surfaces of the pier and plate P2 would be perfectly flat. The extent to which these ideal conditions are not met determines the amount of flange distortion and consequent storage of elastic energy that occur when the flanges are tightened down during assembly. Such a condition is said to be semikinematic,¹ but it is, of course, the usual one due to the inevitability of machining tolerances. With good machine tools, a tolerance on length of less than 0.003 inch should be available. The flatness of the pier was ensured by machining the top surface after completion of all welding. The horizontality of the X_c motion (discussed below) depends entirely on the precision with which plate P2 is leveled. This is controlled by shimming at the base of the support pier.

3. MIRROR MOUNT DESIGN

Of the total of three possible degrees of angular freedom, we require adjustment about two axes, namely, azimuth and elevation. The two classic approaches to this problem are the use of (a) gimbals, and (b) adjustable footscrews. Due to the heavy weight (20 kg) and the considerable size of the mirror, it is difficult to design a mount using gimbals without incurring a heavy space penalty. Also, if the coolant hoses attach to the mirror through its edge surfaces, it is likely they will interfere with the action of the gimbals. For these reasons, consideration of an arrangement involving gimbals was dropped, and the footscrew approach became the preferred method.

Instead of the more usual practice of placing the footscrews in a vertical plate, they are positioned in a horizontal plate as illustrated in Fig. 3. Footscrews A and B are situated on either side of the mirror, while C is directly behind it at a distance of 38 cm. Altitude angle is adjusted by rotation of footscrew C.

Azimuth adjustment of mirror position is provided by rotation of plate P1 relative to plate P2. This is done by locating footscrew A in a conical hole in P2 so that it acts as a pivot. Plastic slipper discs of

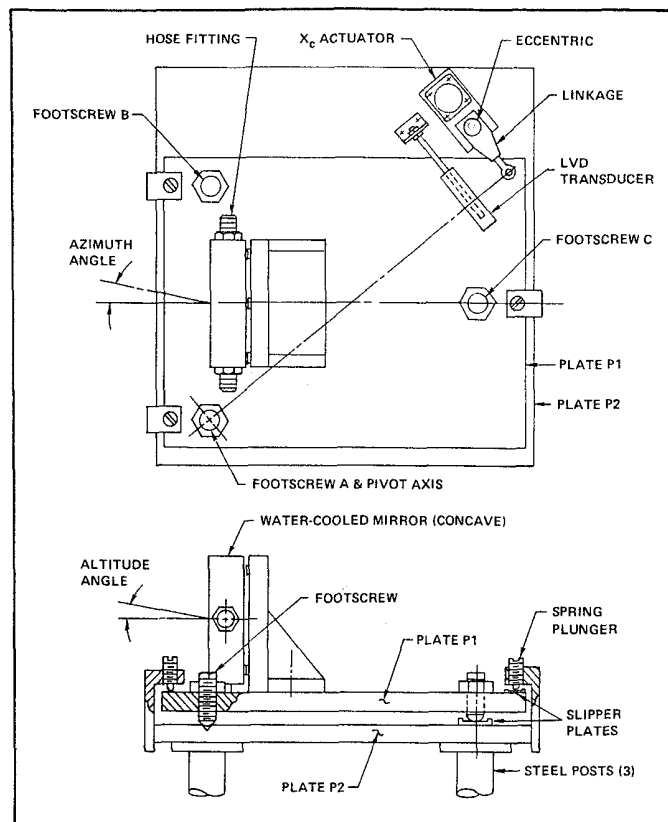


Fig. 3. Mirror mount details.

Delrin-AF² (which contains teflon) are placed under the tips of B and C footscrews to minimize friction. Positive contact against plate P2 is maintained by preload forces supplied by spring plungers in the vicinity of each footscrew. The use of slipper discs limits frictional resistance which the actuator must overcome to a value of 9 kg.

There are important advantages in the mounting method of Fig. 3. One is that the weight of the mirror is supported by pads directly beneath it; this is in contrast to a cantilever suspension which is unavoidable when footscrews lie in a vertical plate. The disadvantage of cantilevering is that the gravity vector of the mirror and the hose forces, both of which can be large in this application, tend to displace the footscrews laterally, making it necessary to offset these forces with stronger preload springs. In Fig. 3, the weight of the mirror (20 kg) and of plate P1 (10 kg) act in the same direction as the spring plungers so that, to a large extent, the assembly is self-preloading.

Another advantage is the relatively long separation between the footscrews in plate P1. The 38 cm lever arm extending from the axis passing through footscrews A and B to footscrew C results in sensitive control of altitude angle. A 1° rotation of C, having 12 threads per cm, rotates the mirror through one arcsecond. The long footscrew separation also contributes to the sensitivity of the X_c transducer, a linear variable differential (LVD) transformer, by maximizing the radial distance at which it operates.

In Fig. 3 the placement of the footscrews in a horizontal plate means that they do not compete with the mirror bracket for space immediately adjacent to the back surface of the mirror. This leads to a design of less complication. There is the added bonus that equal rotations of all footscrews provide vertical translation adjustment which is needed when placing the center of the mirror aperture at the same height as the nozzle centerline.

4. ANALYSIS OF OFFSET PIVOT GEOMETRY

In closed cavity power testing the output power is measured as a function of the distance from the nozzle face to the axis of the

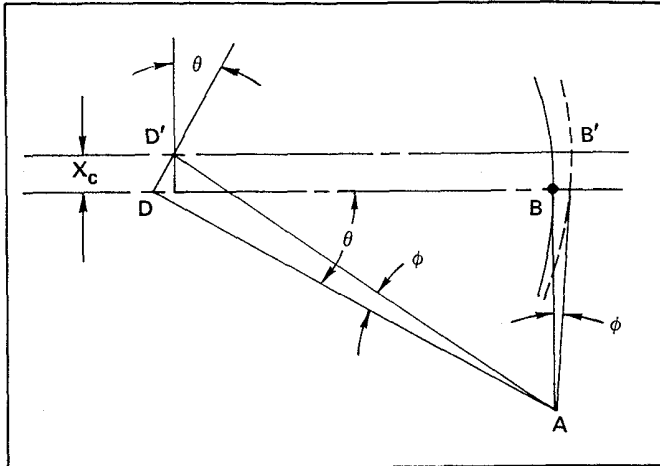


Fig. 4. Offset pivot geometry.

resonator cavity, known as X_c . A convenient method³ of varying X_c is rotating the concave resonator mirror through a small range of azimuth angle and, consequently, there is a need to remotely actuate and measure mirror rotation. The X_c actuator is shown in Fig. 3 attached to one end of plate P1 by a linkage arm by means of which the plate and mirror are rotated about footscrew A acting as pivot.

We can analyze the geometry of the offset pivot by reference to Fig. 4. The initial position of the resonator axis coincides with mirror radius BD, the center of curvature lying at D. Let A be the chosen position for the pivot on line AB which is tangent to the mirror at B. Let ϕ be a small rotation of the mirror, usually less than 1° . During rotation ϕ , the center of mirror curvature moves from D to D', and the resulting position of the resonator axis is B'D' at a distance X_c from the nozzle face. Then, from the diagram we have

$$X_c = DD' \cos \theta = (AD \tan \phi) (\cos \theta) = \frac{(BD \tan \phi) (\cos \theta)}{\cos \theta} \\ = BD \tan \phi.$$

But $BD = R_m$, the mirror radius, and $\tan \phi = \phi$ for small angles. It follows that

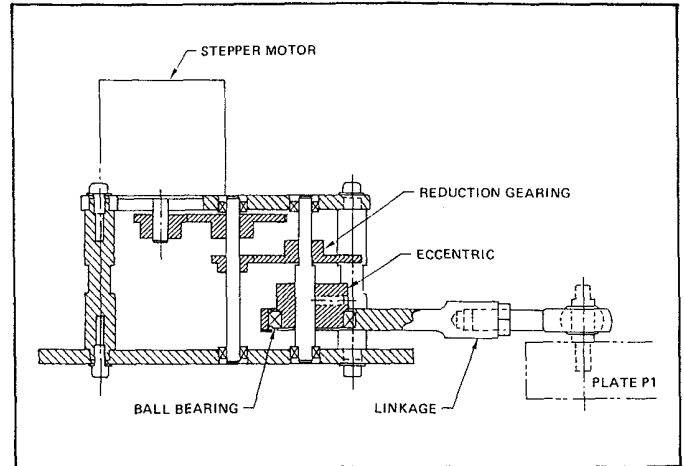
$$X_c = R_m \phi. \quad (7)$$

Although this result indicates that X_c is independent of offset distance AB, a small second order error remains. If, in Fig. 4, DD' were drawn as a circular arc, there would be a component of motion subtracting from X_c having a magnitude of $1/2 (AB) \phi^2$ derived from the formula for the sagitta of an arc. Normally this expression will have a very small value so long as ϕ is a small angle and AB is the order of a mirror width. Consequently, the calibration of X_c instrumentation continues to be based on the measurement of only two parameters, R_m and ϕ , both of which are optical measurements that can be made with high accuracy.

If, due to assembly tolerances, the pivot point does not fall on line AB, the error in X_c is ϕP where P is the perpendicular distance from the pivot to AB, irrespective of the amount of offset. For example, if $P = 2$ mm and $\phi = 0.015$ radians, then $\phi P = .03$ mm, which would normally be a very small percent of X_c .

5. X_c ACTUATION

The rotary motion of plate P1 about footscrew A results from the rotation of an eccentric driven by the actuator motor. It can be seen

Fig. 5. X_c actuator mechanism.

in Fig. 5 how a ball bearing situated between the eccentric and the linkage creates a connection with low backlash and friction. A lead-screw or rack-and-pinion mechanism might have been used to provide the motion; however, it has been found that the eccentric drive is particularly well suited to the needs of chemical laser testing for the following reasons:

1. The two dead-center positions of the eccentric, 180° apart, define the end limits of the X_c excursion. Once the excursion corresponding to a particular eccentric has been calibrated, it is impossible for that calibration to deteriorate because it is cut in hard metal. If a different excursion is required, another eccentric is easily made.
2. One hazard of laser power testing is that if X_c is accidentally made too small, the nozzle can suffer thermal damage. To prevent X_c from reaching a value below the safe minimum, one of the dead-center positions can be used as a dependable end-stop at the upstream end of the excursion.
3. We have found that the nonlinearity of the eccentric drive is not a significant disadvantage since it is present only in the actuation of X_c , not in its measurement. The separation of actuation from measurement makes it possible to tolerate both backlash and nonlinearity in the actuator. The LVDT transducer, on the other hand, is linear, accurate, and totally free of backlash.
4. During calibration of X_c , or in subsequent checking, the two dead-center positions can be accurately judged without special equipment by visual observation of the rotational position of the eccentric. This is due to the slow change of X_c as a function of eccentric rotation near the two ends of the motion, and is a great convenience in the day-to-day operation of the test cell. Calibration of the X_c transducer is by accurate measurements of R_m and ϕ , then substituting in Eq. (7). Angle ϕ is measured in the calibration process by placing a flat, auxiliary mirror on plate P1, then measuring its rotation by means of an autocollimating theodolite having an accuracy of one arcsecond.
5. The eccentric mechanism is highly suitable for driving a member such as plate P1 moving on a circular path. This is in contrast with a leadscrew or rack-and-pinion, the output members of which must follow a strictly rectilinear path.

6. REFERENCES

1. Whitehead, T. N., *The Design and Use of Instruments and Accurate Mechanism*, Dover Publications Inc., New York (1954).
2. Delrin is a trademark of DuPont Corporation, Wilmington, DE.
3. Spencer, D. J., Durran, D. A., and Bixler, H. A., *Appl. Phys. Lett.* 20, 164(1972).